A BIAXIAL ENDURANCE CRITERION DEVELOPED WITHIN THE LINEAR ELASTIC FRACTURE MECHANIC FRAMEWORKS

R. de Moura Pinho[1], S. Pommier[2], C. Mary[3], A. Longuet[4] and F. Vogel[5]

[1] LMT, ENS-Cachan, 61 av. du Président Wilson, 94235 Cachan, France, moura@lmt.ens-cachan.fr.
[2] pommier@lmt.ens-cachan.fr.
[3] SNECMA VILLAROCHE, Rond-Point René Ravaud, 77550 Moissy-Cramayel, France, caroline.mary@snecma.fr.
[4] arnaud.longuet@snecma.fr.
[5] TURBOMECA, F-64511, Bordes, France, François.VOGEL@turbomeca.fr.

ABSTRACT. *A multiaxial fatigue criterion that takes explicitly into account the defect size was developed in a previous study [1]. The material is assumed to contain defects modeled as cracks. The criterion is developed within the LEFM frameworks. Non-singular terms in the asymptotic developments of stresses at crack tip were considered. A critical elastic distortional energy is used as a yield criterion for the crack tip region. The elastic domain of the crack tip region is viewed as an endurance domain in fatigue. With this approach, the defect size effect in the Kitagawa and Takahashi diagram [2] and the hydrostatic stress dependency in the Dang Van [3] criterion are both successfully reproduced. In a previous study [4] a new methodology based on FE computations was developed in order to determine the elastic domain of a material containing a crack in a (K_I, T) diagram. The yield surface as determined from FE computations was shown to provide a good estimate of the experimental endurance limit as well for HCF load as for CCF load. Besides, the influence of the material constitutive behavior on the endurance limit of the material was studied numerically by assuming various constitutive equations, elastic ideally plastic behaviors, linear hardening and the material behavior identified for a Ti-6Al-4V alloy. Results are post-processed to generate Dang Van and Haigh diagrams, yielding satisfactory results.*

INTRODUCTION

In a defect free material, fatigue damage is usually found, according to Miller [5, 6], to occur within secluded grains favorably oriented for plastic slip. Well below the macroscopic yield stress, a grain can cyclically plastically deform and form intrusions and extrusions at the surface, if the maximum resolved shear stress amplitude in that grain exceeds the crystallographic yield stress. A micro-crack can then initiate and propagate until the complete degradation of the structure.

If the material contains defects, fatigue damage is promoted in their vicinity by the same mechanism. However, since defects can act as stress-raisers, fatigue damage takes usually place below the endurance limit of the defect free material [2, 7, 8] and [9]. However, it was shown by Kitagawa and Takahashi [2] that the fatigue limit is reduced by the presence of a defect only if the size of that defect exceeds a transition length defined by the empirical equation of El Haddad et al [7]. Above the transition length, LEFM applies and the defect can be considered as a crack, with a size ($\sqrt{}$ area) defined by Murakami et al. [9] as the square root of the projected area of the defect in the plane that sustains the maximum principal stress.

Billaudeau [8] performed experiments on specimens in C36 Steel that contained manufactured defects with different sizes and geometries. Their results showed that the defect can be considered as a crack and characterized by the $\sqrt{}$ area parameter provided that the stress concentration factor K_t exceeds 2. Thieulot [1] showed that the small crack effect could be described by considering not only the stress intensity factor (SIF) K_I but also the T-stress (the fisrt non-singular term of the elastic field at the vicinity of the crack tip) because of the scale effect induces by this one. For this reason, in the following defects are modeled as cracks so as to formulate a biaxial fatigue criterion that takes into account defects. In this approach, the finite element (FE) method is used to determine the elastic domain of the crack tip region for a given elastic plastic behaviour of the material. The elastic domain is then viewed as an endurance domain in fatigue. It is important to mention that in both cases the frontier of the domain is conventional. The frontier of the elastic domain is defined through an offset that is adjusted using the non propagation threshold SIF of the material ΔK_{th}. The elastic domain of the crack tip region is provided in terms of LEFM quantities. So as to express it in terms of fatigue quantities an additional parameter is required (a crack length a_0) which is adjusted using the fatigue strength at 10^6 cycles.

1 DETERMINATION OF THE ELASTIC DOMAIN

1.1 Stress intensity factor, T-stress and critical plane

So as to express the stress intensity factor, it is assumed that the crack is a penny-shaped crack embedded in an infinite body lying in a plane defined by its normal $\underline{n}$. Let consider a point of the crack front defined by its normal $\underline{t}$. Let σ_n^∞ be the normal stress and σ_t^∞ be the projection of the stress tensor along the axe parallel to the crack plane.

According to Wang [10], we have:

$$K_I = \frac{2}{\pi}.\sigma_n^\infty.\sqrt{\pi.a} \quad T = \sigma_t^\infty - \frac{1+2.\nu}{2}.\sigma_n^\infty \quad with \quad \sigma_n^\infty = \left(\underline{\underline{\sigma}}.\underline{n}\right).\underline{n} \quad \sigma_t^\infty = \left(\underline{\underline{\sigma}}.\underline{t}\right).\underline{t} \qquad (1)$$

These formulas allow to show the scale effect introduced by the non-singular term. Indeed the SIF depends on the crack geometry while the other doesn't. This could

explain why the fatigue strength doesn't depend on the crack size when this one becomes small enough [2].

We assume that the crack plane is that one that sustains the maximal principal stress. Indeed, there is always a potential site for initiation of cracks oriented in this direction provided that the material contains enough grains.

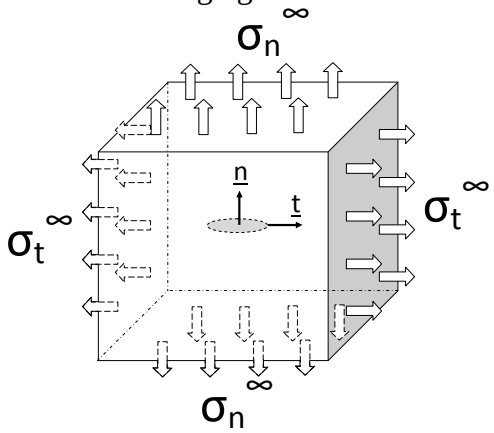

Figure 1. Schematic of a straight crack front in an infinite body

1.2 Research of the endurance domain by FE method

We assume that the material obeys the Von Mises yield criterion, which is a critical distortional energy density criterion. We also consider that the load applied in the case of a material which contains a crack is described by the SIF and the T-stress to account for the scale effect. The residual stress at the vicinity of the crack tip is described by the displacement of the elastic domain in the (K_I, T) plane. Therefore the location (K_{IX}, T_X) of the center of the yield locus of the crack tip region is defined has an internal variable.

In order to express the evolution law of (K_{IX}, T_X) with plastic deformation, variables should be introduced so as to characterize plastic deformation within the plastic region at the global scale. The velocity field in a domain around the crack tip is determined using the FE method and then partitioned by some formulas [4], into discontinuous field through the crack plane (associated with K_I) and continuous component (associated with T-stress) and then finally projected onto a basis of reference fields for each mode.

That basis contains an elastic reference fields, solutions of an elastic FE computation for either K_I or T-stress equal to 1 MPa.m$^{1/2}$ and 1 MPa respectively, and two plastic fields obtained using a proper orthogonal decomposition, after the partition onto continuous and discontinuous field through the crack plane, and non-dimensioned so that their intensity factor, ρ_I and ρ_T, could be read respectively as the CTOD and the crack widening by plastic deformation.

The formulas of the partition onto discontinuous and continuous fields are [4]:

$$2.\tilde{v}_X^I\left(\underline{x},t\right)=\left(v_r^{EF}\left(r,\theta,t\right)-v_r^{EF}\left(r,\pi-\theta,t\right)\right)+\left(v_X^{EF}\left(r,\theta,t\right)+v_X^{EF}\left(r,\pi-\theta,t\right)\right) \quad (2)$$

$$2.\tilde{v}_Y^I\left(\underline{x},t\right)=-\left(v_\theta^{EF}\left(r,\theta,t\right)+v_\theta^{EF}\left(r,\pi-\theta,t\right)\right)+\left(v_Y^{EF}\left(r,\theta,t\right)-v_Y^{EF}\left(r,\pi-\theta,t\right)\right) \quad (3)$$

$$2.\tilde{v}_X^T\left(\underline{x},t\right)=-\left(v_r^{EF}\left(r,\theta,t\right)-v_r^{EF}\left(r,\pi-\theta,t\right)\right)+\left(v_X^{EF}\left(r,\theta,t\right)-v_X^{EF}\left(r,\pi-\theta,t\right)\right) \quad (4)$$

$$2.\tilde{v}_Y^T\left(\underline{x},t\right)=\left(v_\theta^{EF}\left(r,\theta,t\right)+v_\theta^{EF}\left(r,\pi-\theta,t\right)\right)+\left(v_Y^{EF}\left(r,\theta,t\right)+v_Y^{EF}\left(r,\pi-\theta,t\right)\right) \quad (5)$$

where v_r^{EF} and v_θ^{EF} are the components of the velocity field in a polar basis. The continuous part is associated with the T-stres and the ρ_T contributions and the discontinuous with K_I and ρ_I.

Finally at each time increment the velocity field $v^{EF}\left(\underline{x},t\right)$ is approached by either by an elastic projection $\tilde{v}^e\left(\underline{x},t\right)$ or by an elastic plastic projection $\tilde{v}^e\left(\underline{x},t\right)+\tilde{v}^i\left(\underline{x},t\right)$:

$$\underline{v}^{EF}\left(\underline{x},t\right)=\underbrace{\left(\frac{d\tilde{K}_I}{dt}(t).\underline{u}_I^e\left(\underline{x}\right)+\frac{d\tilde{T}}{dt}(t).\underline{u}_T^e\left(\underline{x}\right)\right)}_{\underline{\tilde{v}}^e\left(\underline{x},t\right)}+\underbrace{\left(\frac{d\rho_I}{dt}(t).\underline{u}_I^i\left(\underline{x}\right)+\frac{d\rho_T}{dt}(t).\underline{u}_T^i\left(\underline{x}\right)\right)}_{\underline{\tilde{v}}^i\left(\underline{x},t\right)} \quad (6)$$

With that approach ρ_I and ρ_T are a condensed measure of the plastic deformation rate within the crack tip region. The relative error between the calculated velocity field and the approached one is defined respectively by C_{1R}, if an elastic approximation is used and by C_{2R} if and elastic plastic approximation is used:

$$C_{1R}\left(t_n\right)=\frac{\int_\Omega\left(\Delta\underline{v}_I^{EF}\left(r,\theta,t_n\right).\left(t_{n+1}-t_n\right)-\Delta\underline{u}^e\left(r,\theta,t_n\right)\right)^2 dS}{\int_\Omega\left(\Delta\underline{v}_I^{EF}\left(r,\theta,t_n\right).\left(t_{n+1}-t_n\right)\right)^2 dS} \quad (7)$$

$$C_{2R}\left(t_n\right)=\frac{\int_\Omega\left(\Delta\underline{v}_I^{EF}\left(r,\theta,t_n\right).\left(t_{n+1}-t_n\right)-\Delta\underline{u}^e\left(r,\theta,t_n\right)-\Delta\underline{u}^i\left(r,\theta,t_n\right)\right)^2 dS}{\int_\Omega\left(\Delta\underline{v}_I^{EF}\left(r,\theta,t_n\right).\left(t_{n+1}-t_n\right)\right)^2 dS} \quad (8)$$

If $C_{1R} = C_{2R}$ an elastic approximation is just as precise as an enriched one, the crack tip region is considered as elastic. With that criterion it is possible to determine from the results of FE computations, the frontier of the elastic domain, for various histories and loading directions, and therefore to find the position (K_{IX}, T_X) of the centre of the elastic domain and its evolution with ρ_I and ρ_T. For more details see [4].

2 RESULTS

2.1 Identification of ΔKI_{TH} for different elastic-plastic constitutive laws

The material used for this study is a titanium alloy (Ti-6AL-4V) for which the elastic-plastic constitutive law had been identified by Le Biavant-Guerrier [11].

The yield criterion is $f = 0$ where:

$$f = \left| \underline{\underline{S}} - \underline{\underline{X}} \right| - R \tag{9}$$

$$R = R_O + Q.\left(1 - e^{-b.p}\right) \tag{10}$$

$$\dot{\underline{\underline{X}}} = \frac{2}{3}.C.\dot{\varepsilon}_P - \gamma.\underline{\underline{X}}.p \tag{11}$$

where $\underline{\underline{S}}$ is the deviatoric stress tensor, $\underline{\underline{X}}$ is the centre of the elastic domain, R is the size of the elastic domain and p is the cumulated strain. The material parameters are gathered in Table 1. This material model will be noted model (1) in the following.

Table 1: Ti-6AL-4V material data [11].

E (GPa)	ν	R_O (MPa)	Q (MPa)	b	C (MPa)	γ
119	0,29	800	-240	9	105000	300

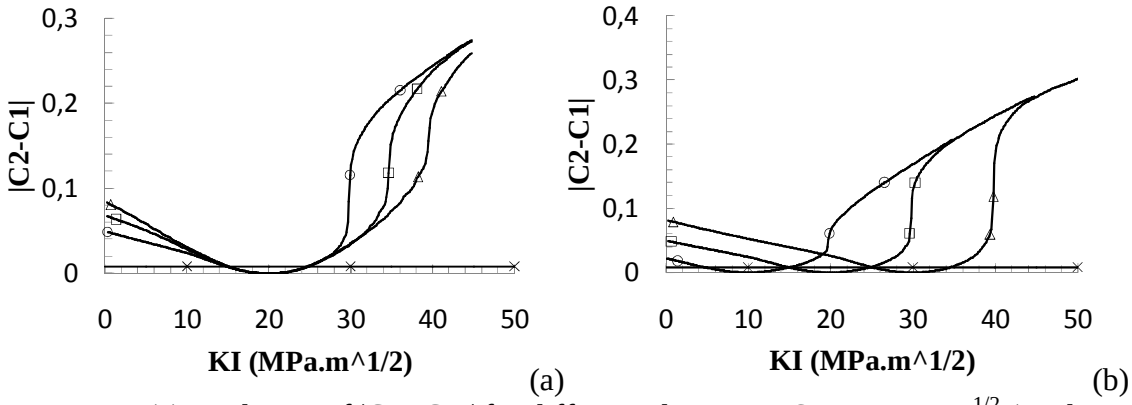

Figure 2. (a) Evolution of $|C_{2R}\text{-}C_{1R}|$ for different alternating SIF in MPa.m$^{1/2}$ (circle – 10, square - 15 and triangle - 20) in the case of a mean SIF equal to 20 MPa.m$^{1/2}$, (b) Evolution of $|C_{2R}\text{-}C_{1R}|$ for different mean SIF in MPa.m$^{1/2}$ (circle –10, square - 20 and triangle - 30) in the case of an alternating SIF equal to 10 MPa.m$^{1/2}$.

To identify the criterion, the FE model is subjected to 30 decreasing uniaxial load cycles in mode I for differents average and alternating stress, so that the material reaches its saturation regime in the crack tip region. For this material, the non propagation threshold is equal to ΔKIth=10 MPa√m. The value of |C1R-C2R|, is therefore adjusted at 8.10-3 so that the yield point corresponds to the non propagation threshold when material hardening is saturated (Figure 2-a). For all mean values of load and initial amplitude of load, the value of |C1R-C2R| is always the same to reach ΔKIth.

This work had also been done for different elastic plastic constitutive laws in order to study their influence on the Haigh diagrams. The parameters of the models are summarizing on Table 2. Figure 3 shows the hardening behaviour of these models in the case of a tension load. The different models were chosen to frame the material behavior identified.

Table 2: Some elastic-plastic constitutive laws which bound the reference behaviour

Elastic-plastic constitutive laws	E	ν	Ro	C	|C2R-C1R|
Elastic ideally plastic with yield stress equal to the yield stress of the material (2)	119000	0,29	800	1	0,01
Elastic ideally plastic with yield stress equal to the maximum stress of the material (3)	119000	0,29	1120	1	0,005
Kinematic hardening (4)	119000	0,29	800	30164	0,005

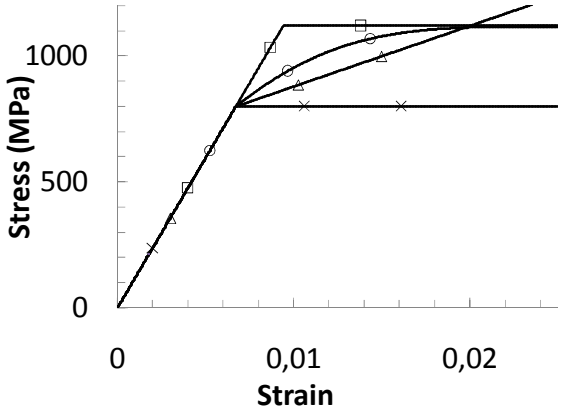

Figure 3. Elastic plastic constitutive laws simulations in the case of a tension load (circle – model (1), cross – model (2), square – model (3) and triangle – model (4)).

2.2 Post-processing in a shear stress / hydrostatic pressure diagram

In order to identify the crack length a_0 of the criterion, the frontier of the elastic domain for a load ratio equal to -1 is plotted in a shear stress / hydrostatic pressure diagram for different crack length (a cylindrical crack is considered [10]). The frontier of the elastic domain is compared with the Dang Van curve and it is assumed that a_0 is the crack length for which the distance between them is minimal (Figure 4-a). We can also plot the evolution of the elastic domain for different load ratios (Figure 4-b).

In Figure 5, the borders of the elastic domain for a chosen mean SIF and for different material constitutive laws are plotted. This diagram shows the high importance of well describing the material behavior to obtain representatives results. Indeed, the size of the elastic domain (fatigue strength) depends on the constitutive law chosen.

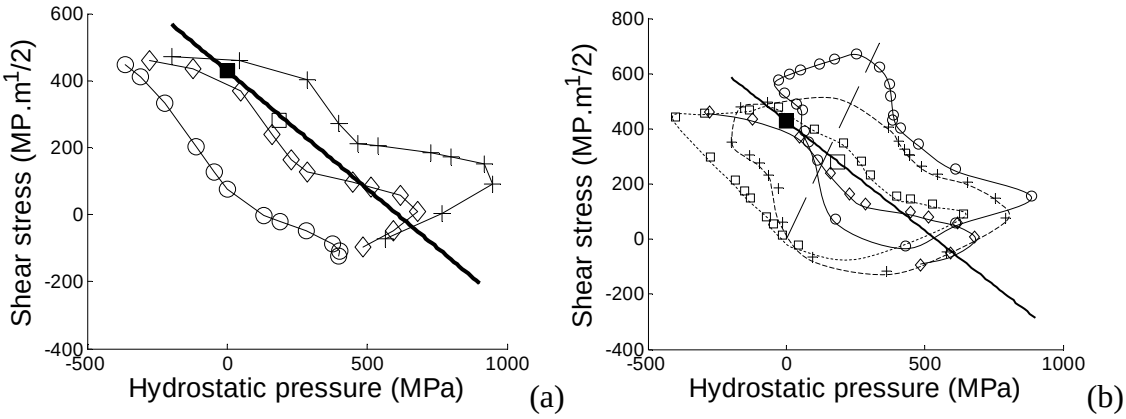

Figure 4. (a) Elastic domain for different crack length (circle – 50 μm, diamond – 150 μm and cross – 5 mm) obtained with model (1). Comparison with the Dang Van criterion [3] (empty square – fatigue strength in tension: 560 MPa and full square – fatigue stress in torsion: 411 MPa [12])
(b) Position of the elastic domain for different mean SIF and T-stress (diamond – K_I=0 MPa.m$^{1/2}$ – T=0 MPa, square – K_I=3 MPa.m$^{1/2}$ – T=-230 MPa, cross – K_I=7 MPa.m$^{1/2}$ – T=-537 MPa and circle – K_I=10 MPa.m$^{1/2}$ – T=-766 MPa). The direction of the load is plotted in dashed line.

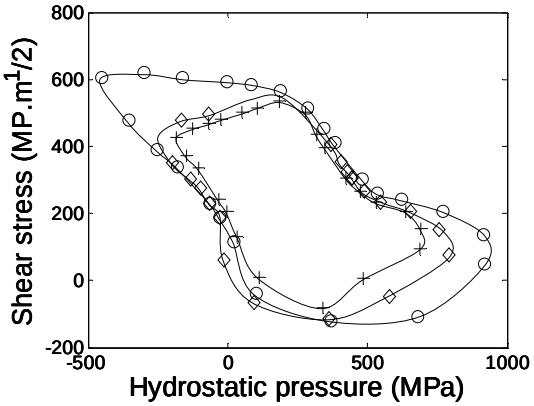

Figure 5. Comparison of the yield surfaces of the crack tip region, for a set of different material constitutive laws. The mean SIF is 7 MPa.m$^{1/2}$, and the mean T-stress is -537 MPa (diamond – model (1), cross – model (2) and circle – model (3)).

2.3 Building Haigh diagrams

With Eq. 1 and by knowing the evolution of the center of the elastic domain, one can plot a Haigh diagram for which the stress is defined as the normal stress of the crack plane. We may note the strong influence of the constitutive law on the curve in Figure 6. It seems that the curve which most fit the experimental curve is that corresponding to law identified for the material. However, Haigh diagram shown (Figure 6-b) does not correspond to the material studied, so only trends can be compared. Furthermore, the simulated loading is not a tension load (see Figure 4-a).

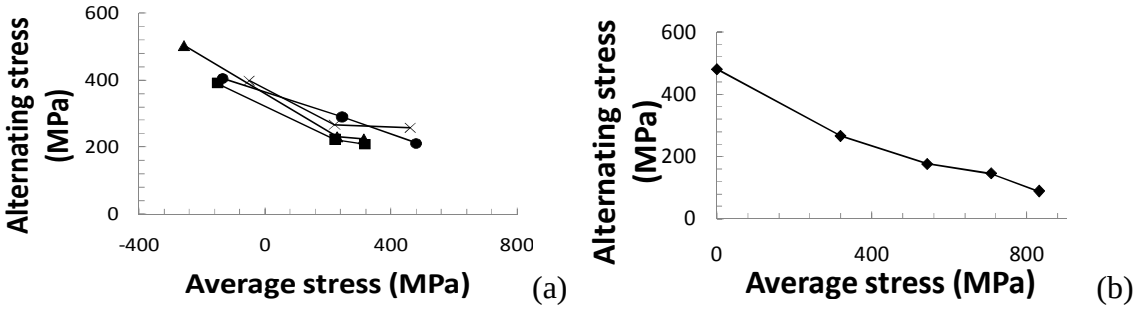

Figure 6. (a) Haigh diagram generated for different material constitutive laws (circle – model (1), square – model (2), triangle – model (3) and cross – model (4)). (b) Experimental Haigh diagram in tension load [13] for a Ti-6Al-4V alloy.

CONCLUSION

A method was developed to determine the endurance domain in fatigue from FE analyses. The elastic domain is viewed as an endurance domain in fatigue. The frontier of the elastic domain is defined through an offset that is adjusted using the non propagation threshold SIF of the material ΔKth. It was shown that the same offset can be used whatever the mean SIF, or the initial SIF loading amplitude.

The elastic domain of the crack tip region is provided in terms of LEFM quantities. So as to express it in terms of fatigue quantities an additional parameter is required (a crack length) which is adjusted using the fatigue strength at 10^6 cycles, for the TiAl4V titanium alloy, a crack length of 150µm was identified. Once identified the parameters can be used to determine the endurance domain (a 10^6 cycles fatigue life) for various loading histories. For instance, the post-treatment routine shows that a mean stress effect can be viewed as a displacement of the endurance domain. This result is very useful to predict the fatigue strength in LCF+HCF conditions.

REFERENCES

1. Thieulot, E., Pommier, S., Fréchinet S. (2006) *ESMC 2006 – 6th Eur. Solid Mech. Conf.*
2. Kitagawa, H., Takahashi, S. (1976) *2nd Int. Conf. Mech. Behaviour of Mat., 627-631*.
3. Dang Van, K., Le Douaron, A., Lieurade, H.P. (1984) *6th Int. Conf. Frac., 1879-1885*.
4. De Moura Pinho, R., Pommier, S., Longuet, A., Mary, C., Vogel, F. (2009) *Fatigue Design 2009*.
5. Miller, K.J. (1987) *Fatigue Fract. Eng. Mat. Struct.*, **10**, 75-91.
6. Miller, K.J. (1987) *Fatigue Fract. Eng. Mat. Struct.*, **10**, 93-113.
7. El Haddad, M.H., Topper, T.H., Smith, K.N. (1979) *Eng. Fract. Mech.*, **11**, 573-584.
8. Billaudeau, T., Nadot, Y., Bezine, G. (2004) *Acta Materialia*, **52**, 3911-3920.

9. Murakami, Y., Endo, M. (1986) *Effects of hardness and crack geometries on ΔK_{th} of small cracks emanating from small defects. The behavior of short fatigue cracks*, pp. 275-293, K.J. Miller and E.R. de los Rios (Eds), Mech. Eng. Publications, London.
10. Wang, X., (2004) *Eng. Fract. Mech.*, **71**, 2283-2298.
11. Le Biavant-Guerrier, K., (2000) Msc Thesis, Ecole Centrale de Paris, Paris.
12. Delahay, T., (2004) Msc Thesis, Université de Bordeaux I, Bordeaux.
13. Lanning, D.B., Nicholas, T., Haritos, G.K. (2005) *Int. J. Fat.*, **27**, 45-57.